

**CASE REPORT****A Rare Case of Concordant Atrioventricular Connection to L-Looped Ventricles in Situs Solitus: 4-Dimensional Magnetic Resonance Imaging and 3D Printing**Gregory Perens<sup>1,\*</sup>, Takegawa Yoshida<sup>2</sup> and J. Paul Finn<sup>2</sup><sup>1</sup>UCLA Mattel Children's Hospital, Children's Heart Center, Los Angeles, CA, USA<sup>2</sup>Diagnostic Cardiovascular Imaging Laboratory, Department of Radiology, 12222 David Geffen School of Medicine at UCLA, Los Angeles, CA, USA

\*Corresponding Author: Gregory Perens. Email: gperens@mednet.ucla.edu

Received: 05 February 2022 Accepted: 24 May 2022

**ABSTRACT**

An infant male presented with the rare anatomy consisting of situs solitus, concordant atrioventricular connections to L-looped ventricles, double outlet right ventricle (DORV), and hypoplastic aortic arch. 6 months after neonatal aortic arch repair, the morphologic right ventricle function deteriorated, and surgical evaluation was undertaken to determine if either biventricular repair with a systemic morphologic left ventricle or right ventricular exclusion was possible. After initial echocardiography, magnetic resonance imaging (MRI) was used to create detailed axial and 4-dimensional (4D) images and 3-dimensional (3D) printed models. The detailed anatomy of this rare, complex case and its use in pre-surgical planning is presented.

**KEYWORDS**

Magnetic resonance imaging; cardiac segments; 3D printing

**1 Introduction**

The congenital heart case here presented had the rare anatomy of situs solitus with concordant atrioventricular connections to L-looped ventricles and DORV. Hearts with similar anatomy consisting of mismatching atrioventricular connection and ventricular relationship were previously reported by Wager et al. [1,2], and van Praagh [3]. Anderson et al. [4] also reported a similar case with dextrocardia and left juxtaposition of the atrial appendages describing that there was disharmony between the atrioventricular connections and the segmental combinations. This complex anatomy has previously been demonstrated in the literature using pathologic specimens or 2-dimensional angiographic and echocardiography images. 4-dimensional cardiac MRI and 3D printing may allow for a more complete understanding of the anatomic relations and facilitate clinical decision-making. In this case, the clinical question to be answered was: could the morphologic left ventricle flow be baffled surgically to the right ventricular outflows. 4D MRI images and 3D printed heart models were created and evaluated for surgical planning.

**2 Methods**

Institutional review board approval has been obtained for this study to report the use of 4-dimensional MRI in children. Informed consent for this imaging is obtained from parents prior to obtaining the images. The



patient's chart was reviewed for clinical and MRI data and reported here as a single case report and discussion. 3- and 4-dimensional MRI images and printed heart model shown are those used for clinical care.

### 3 Case Report

A male infant with a prenatal diagnosis of complex double outlet right ventricle and hypoplastic aortic arch was born after 39 weeks of gestation. At birth, he weighed 3700 gm and his oxygen saturation at room air ranged from 90%–95%. A transthoracic echocardiogram demonstrated visceral and atrial situs solitus, levocardia, concordant atrioventricular connections and double outlet right ventricle (DORV) with cardiac segments, {S, L, D}. The atrial appendages were juxtaposed on the right side of the arterial trunks.

The ventricles showed an unusual spatial relationship for the given atrioventricular connection with the morphologically left ventricle positioned anteriorly and the right ventricle posteriorly. A large ventricular septal defect located at the base adjacent to the septal atrioventricular valve leaflets and extending into the muscular septum was remote from both aortic and pulmonary valves. There was a side-by-side great arterial relationship with the aorta on the right. The aortic valve was small, and the aortic arch was hypoplastic. The patient was started on prostaglandin infusion and underwent an aortic arch reconstruction (Damus-Kaye-Stansel/Norwood procedure) with a right ventricle-to-pulmonary artery conduit (Sano procedure) and atrial septectomy on the second day of life. The initial echo after surgery showed good ventricular systolic function and laminar right ventricular outflow with minimal atrioventricular valve regurgitation.

Six months after the surgery, the patient's condition deteriorated with the right ventricular function severely diminished. The right ventricle end-diastolic pressure was 9 mmHg, the mean pulmonary pressure 16 mmHg, and pulmonary: systemic flow ratio 0.3, and no right ventricle outflow gradient was present. Four-dimensional (4D) cardiac magnetic resonance (CMR) imaging was performed using the multiphase, steady-state imaging with contrast enhancement (MUSIC) technique [5,6] on a 3T scanner (Magnetom TIM Trio, Siemens Medical Solutions, Erlangen, Germany) and ferumoxytol (Feraheme, AMAG Pharmaceuticals, Waltham, USA). The 4D MUSIC image data were post-processed for cinematographic visualization and 3D modeling and printing of the end-diastolic phase.

The 4D MUSIC CMR confirmed the echocardiographic diagnosis with a clear demonstration of the complex pathologic features of the case (Figs. 1 and 2) and Video 1. There were bilateral superior vena cavae with a small bridging vein. Both systemic and pulmonary veins had usual spatial orientation and normal connections to the right and left atria, respectively. However, the left atrial cavity extended rightward and anteriorly with its outlet and the mitral valve was positioned superior and anterior to the outlet of the right atrium and the tricuspid valve. The left atrial appendage was also displaced rightward to be positioned above and slightly anterior to the right atrial appendage. The morphologically left ventricle was located anterior to the inlet and trabecular parts of the morphologically right ventricle. The right ventricle consisted of the inlet component on the right, the apical trabecular part on the left above the diaphragm, and the outlet superiorly on the left (Fig. 1B). The ventricular septum was in an oblique coronal plane facing the anteriorly located left ventricle. Thus, the ventricular relationship was consistent with that of the L-looped ventricles (Fig. 1A), and the internal topological arrangement of the right ventricle was consistent with a left-hand pattern, i.e., the right ventricular septal surface accepted the palm of the observer's left hand with the thumb placed toward the tricuspid valve orifice and the fingers toward the outlet (Fig. 1B). Therefore, there was a mismatching L-loop ventricular relationship and left-hand ventricular topology for the setting of concordant atrioventricular connection in situs solitus. Despite the very unusual atrial and ventricular relationships, the atrioventricular connection axes were parallel (Figs. 1C and 2C). Both the aorta and pulmonary arterial trunks arose from the right ventricle through the bilateral muscular infundibula. There was a large ventricular septal defect at the base that was remote from both arterial valves. The subaortic outflow tract and aortic valve were small. The subaortic outflow

tract showed dynamic narrowing. The great arteries were related side-by-side with the aorta on the right side of the pulmonary arterial trunk. The right ventricle-to-pulmonary artery conduit was small but patent. The reconstructed aortic arch was unobstructed.

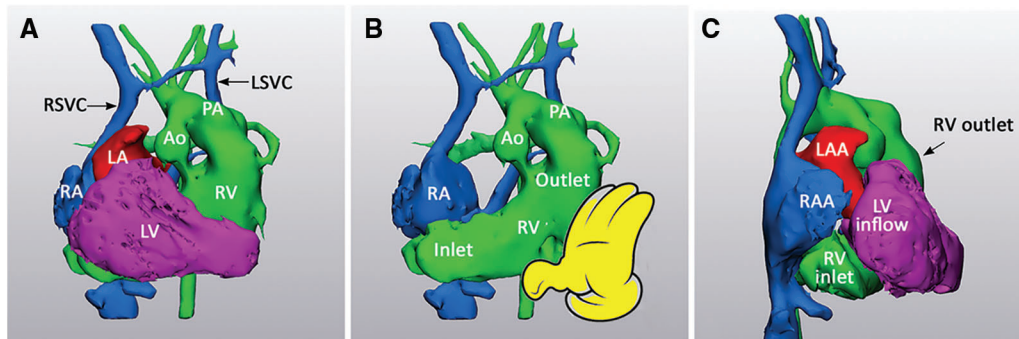


**Figure 1:** 3D volume-rendered angiograms obtained in diastole. A. Frontal view demonstrates the segmental setting {S, L, D}. The outlet of the left atrium (LA) is located anteriorly and superiorly in relation to the right atrium (RA). The left atrium is connected to the anteriorly located morphologically left ventricle (LV). The right ventricular (RV) inlet and apical trabecular parts are located posterior to the left ventricle. Both arterial trunks arise from the right ventricle through the muscular infundibula. The aorta (Ao) and the pulmonary arterial trunk (PA) are surgically connected. B. Frontal view obtained after removal of the left atrium and ventricle shows the right atrium connecting to the right ventricle and the septal surface of the right ventricle facing forward. The septal surface accepts the palm of the observer’s left hand with the thumb directed toward the right ventricular inlet and the fingers directed toward the right ventricular outlet. C. Right anterior oblique view shows the juxtaposed right (RAA) and left (LAA) atrial appendages on the right side of the arterial trunks. The atria connect to the underlying ventricular inlets in a parallel fashion in this particular view. Abbreviation: LSVC, left superior vena cava; RSVC, right superior vena cava

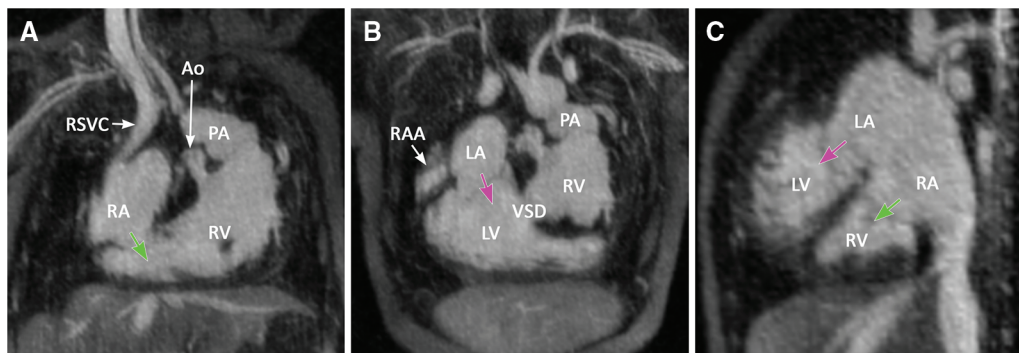


**Figure 2:** Maximum intensity projection images were reconstructed in oblique coronal planes across the tricuspid (A) and mitral (B) valves, and oblique sagittal planes across both tricuspid and mitral valves (C). There is a concordant atrioventricular connection through the parallel mitral (pink arrow) and tricuspid (green arrow) valves. The mitral valve is located superiorly and anteriorly in relation to the tricuspid valve. A large ventricular septal defect (VSD) is seen between the inlet parts of the ventricles. It is remote from both arterial valves

Due to the deterioration of the right ventricle function, the only surgical options considered were biventricular repair with a systemic left ventricle or single ventricle palliation with right ventricle exclusion. A 3D heart model was printed to assess feasibility of routing the anterior morphological left ventricle through the ventricular septal defect to the outflow tract of the right ventricle (Fig. 3). The child was deemed not a surgical candidate because of two factors: (a), the remoteness of the semilunar valves from the ventricular septal defect visualized on the model; (b), the unfavorable location of the septal and anterior leaflets of the tricuspid valve in relation to the VSD shown on MRI axial images. The child underwent successful heart transplantation at the age of 8 months.

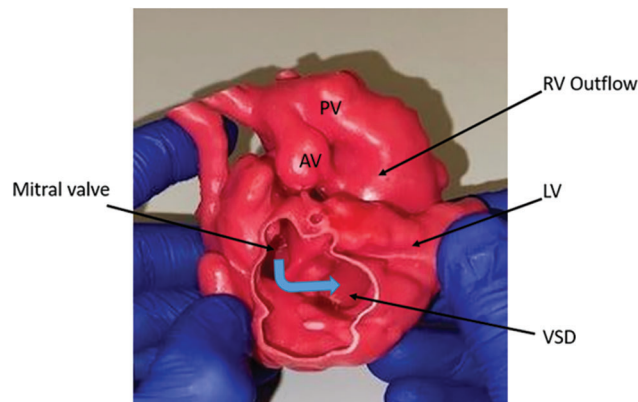


**Figure 3:** 3D printed heart model. The model is hollow shell of the intracardiac blood pool, with the inner surface representing the endocardium. The left ventricle free wall is removed. The blue arrow represents a course from the mitral valve through the ventricular septal defect (VSD) to the right ventricle (RV). AV, aortic valve; LV, left ventricle; PV, pulmonary valve

#### 4 Discussion

High-resolution, 4-dimensional cardiac imaging with 3D printing provided clear visualization of highly complex congenital anatomy. The 3D CMR reconstructions shown here clarify the unusual anatomy, namely L-looped ventricles with concordant atrioventricular connections. The rare anatomy is manifest in parallel, but supero-inferior ventricular inflow connections and ventricles that lead to L-looped ventricles. The right ventricular inlet is inferior to both the left ventricular inlet and apex. Similar anatomy has been described with discordant atrioventricular connections and D-looped ventricles [2,3]. These cases highlight the need to define the atrio-ventricular connections as well as their spatial relations. Ultimately, the clinical question answered using MRI imaging and 3D models was that intracardiac baffle of the anterior morphologic left ventricle to the right ventricular outflows was not possible.

The case described herein is an extremely rare congenital heart disease showing a segmental setting of {S, L, D} with concordant atrioventricular connections between the situs solitus atria and the L-looped ventricles, double outlet right ventricle and right juxtaposition of the atrial appendages. These rare hearts are distinctly different from so called twisted or criss-cross hearts that are also characterized by the unexpected relationship of the cardiac chambers and great arterial trunks but show an expected ventricular loop pattern or right ventricular internal anatomy for the given atrioventricular connection. In other words, the ventricular loop pattern is harmonious with the atrioventricular connection. In contrast to the twisted hearts, the current case showed parallel axes of the tricuspid and mitral valves. Right juxtaposition of the atrial appendage appears to be part and parcel of the rightward and anterior displacement of the left atrial outlet in the current case and the cases reported by Wagner et al. [1] and Seo et al. [2]. Due to the abnormal

supero-inferior relationship between the mitral and tricuspid valves, the left ventricular inlet is located on top of the right ventricular inlet, which has only very rarely been reported [7,8].

Improvements in advanced imaging modalities should facilitate the understanding of such complex congenital hearts and improve the 3D models from which they are created. The MUSIC CMR sequence described here is used in combination with ferumoxytol, an iron-based contrast agent, to create detailed 4D cardiac images that span the cardiac cycle [1,2]. Imaging throughout the entire cardiac cycle provides a 3D overview of the bi-ventricular function and dynamic outflow narrowing and allows for printing of a model at any point in the cardiac cycle.

The usefulness of 3D models for the surgical evaluation of potential bi-ventricular repair of DORV has been well documented in the literature [9–12]. Pre-surgical questions to be answered by inspection of DORV heart models include: will the patch baffle obstruct the right ventricular inflow significantly; is an arterial switch needed to bring the aorta closer to the left ventricle and VSD; and will the VSD need to be enlarged. For the unique DORV anatomy presented here, the 3D model allowed for a pre-operative inspection of the intracardiac relations, beyond what can be assessed with 2D axial images and 3D computer reconstructions.

The main limitations of this report include it being a single case and lacking a review of the pathologic specimen. The authors have only encountered one case with this type of anatomy, and thus a case series was not possible, only a literature review of previous cases. The pathologic specimen was no longer available post-transplant for inclusion in this report. 3D echocardiography was not performed on this patient. For complex anatomy, the authors' preference is to perform 4D MRI, even though it requires anesthesia for imaging of children.

## 5 Conclusion

High-resolution, 4-D MUSIC MRI with 3D printing provides detailed and dynamic visualization of rare, complex pediatric cardiac anatomy, providing unprecedented insight into segment connections and topology.

**Acknowledgement:** The authors would like to thank Dr. Shi-Joon Yoo for his input regarding the pathology of this case.

**Funding Statement:** The authors received no specific funding for this study.

**Conflicts of Interest:** The authors declare that they have no conflicts of interest to report regarding the present study.

## References

1. Wagner, H. R., Alday, L. E., Vlad, P. (1970). Juxtaposition of the atrial appendages: A report of six necropsied cases. *Circulation*, 42(1), 157–163. DOI 10.1161/01.CIR.42.1.157.
2. Seo, J. W., Choe, G. Y., Chi, J. G. (1989). An unusual ventricular loop associated with right juxtaposition of the atrial appendages. *International Journal of Cardiology*, 25(2), 219–233. DOI 10.1016/0167-5273(89)90111-3.
3. van Praagh, R. (1987). When concordant or discordant atrioventricular alignments predict the ventricular situs wrongly. I. Solitus atria, concordant alignments, and L-loop ventricles. II. Solitus atria, discordant alignments, and D-loop ventricles. *Journal of the American College of Cardiology*, 10(6), 1278–1279. DOI 10.1016/S0735-1097(87)80131-6.
4. Anderson, R. H., Smith, A., Wilkinson, J. L. (1987). Disharmony between atrioventricular connections and segmental combinations: Unusual variants of “crisscross” hearts. *Journal of the American College of Cardiology*, 10(6), 1274–1277. DOI 10.1016/S0735-1097(87)80130-4.

5. Han, F., Zhou, Z., Han, E., Gao, Y., Nguyen, K. L. et al. (2017). Self-gated 4D multiphase, steady-state imaging with contrast enhancement (MUSIC) using rotating cartesian K-space (ROCK): Validation in children with congenital heart disease. *Magnetic Resonance in Medicine*, 78(2), 472–483. DOI 10.1002/mrm.26376.
6. Nguyen, K. L., Ghosh, R. M., Griffin, L. M., Yoshida, T., Bedayat, A. et al. (2021). Four-dimensional multiphase steady-state MRI with ferumoxytol enhancement: Early multicenter feasibility in pediatric congenital heart disease. *Radiology*, 300(1), 162–173. DOI 10.1148/radiol.2021203696.
7. Yang, G., Wang, Q., He, J., Wu, M. (2010). Superior left ventricle in combination with inferior right ventricle: Presenting with balanced hemodynamics and mild symptoms in a late adolescent. *Texas Heart Institute Journal*, 37(4), 445–448.
8. Angelini, P. (2010). Left ventricle on top versus right ventricle on top in superoinferior ventricles: What are we talking about? *Texas Heart Institute Journal*, 37(4), 442–444.
9. Yoo, S. J., Hussein, N., Peel, B., Coles, J., van Arsdell, G. S. et al. (2021). 3D modeling and printing in congenital heart surgery: Entering the stage of maturation. *Frontiers in Pediatrics*, 9, 621672. DOI 10.3389/fped.2021.621672.
10. Zhao, L., Zhou, S., Fan, T., Li, B., Liang, W. et al. (2018). Three-dimensional printing enhances preparation for repair of double outlet right ventricular surgery. *Journal of Cardiac Surgery*, 33(1), 24–27. DOI 10.1111/jocs.13523.
11. Yoo, S. J., van Arsdell, G. S. (2018). 3D printing in surgical management of double outlet right ventricle. *Frontiers in Pediatrics*, 5, 289. DOI 10.3389/fped.2017.00289.
12. Bhatla, P., Tretter, J. T., Ludomirsky, A., Argilla, M., Latson, L. A. et al. (2017). Utility and scope of rapid prototyping in patients with complex muscular ventricular septal defects or double-outlet right ventricle: Does it alter management decisions? *Pediatric Cardiology*, 38(1), 103–114. DOI 10.1007/s00246-016-1489-1.